RSC Advances

ROYAL SOCIETY OF CHEMISTRY

www.rsc.org/advances

Influence of hollow carbon microspheres with micro and nano-scale on the physical and mechanical properties of epoxy syntactic foams

Xiudi Li,[a] Ming Zhu,[a] Xuemei Tang,[a] Qingjie Zhang,[a] Xiaoping Yang[a] and Gang Sui*[a]

Abstract: The epoxy syntactic foams were prepared by introducing hollow carbon microspheres (HCMs) with micro and nano-scale. Based on the surface structure analysis of HCMs, the effects of HCM content and particle size on the mechanical properties, dimensional stability, thermal conductivity, thermal stability and dielectric properties of epoxy foam were investigated. The density of the epoxy foam gradually declined with the increase of micro-scale HCM (M-HCM) content up to 9wt%, and the compression strength of epoxy foam just decreased slightly, while the compression modulus and flexural modulus were enhanced continuously. When 0.5wt% and 1wt% HCMs were involved, the reinforcing effect of nano-scale HCM (N-HCM) was superior to the M-HCMs. The compression strengthh of N-HCM/epoxy foams were almost equivalent to the neat epoxy, while the flexural strength of N-HCM samples exhibited an obvious superiority. The dimensional stability and thermal stability of epoxy foams were also improved with the addition of HCMs. Besides, the introduction of the M-HCMs and N-HCMs gave rise to the different effects on the thermal conductivity, electrical conductivity and dielectric constant of the resulting epoxy foams due to the diversity in the interfacial interaction and microstructure. These results indicate that the HCM/epoxy syntactic foams show potential application values in multifunctional materials with lightweight and high rigidity.

Introduction

Syntactic foam is a kind of composite materials consisting of hollow fillers and polymer matrix. In general, the hollow fillers can be made by glass, carbon, ceramics, polymers, and even metals[1,2]. Dispersion of the hollow fillers in a matrix can create a porous material system with closed cell. By changing the amount of hollow particles, different densities and thus microstructure of syntactic foam can be produced[1-3]. syntactic foam has a variety of material feature, including low density, high specific strength, high specific modulus, low moisture absorption, and superior dielectric property, which makes it more suitable for the application in aviation, marine, energy, construction and electronics industries compared to solid particle-filled composites, open cell structured foams, and other low density materials[4-7].

In recent years, many researchers have concerned the investigation of syntactic foam. Thermal properties and electrical properties are important for syntactic foam used as circuit substrates and packaging materials. Yung[8] and Park[9] studied thermal stabilities, dielectric properties of hollow glass microspheres (HGMs) filled epoxy composites. The results showed that the dielectric constant, dielectric loss and the coefficient of thermal expansion (CTE) of the composites decreased simultaneously with increasing HGM content. However, the thermal conductivity of the composites decreased due to the addition of HGMs with inner gas structure. Heat transfer in a timely manner is very critical for electronic materials. The vital issue of preparing syntactic foam with good heat dissipation function is to ensure the high thermal conductivity of the hollow particle fillers. Good mechanical properties are also essential to the application of syntactic foam. Gupta et al.[10-15] studied the mechanical properties of different kinds of hollow glass particles filled vinyl ester resin. The results suggested that the mechanical properties of the syntactic foam were dependent on the type of the hollow particles, and decreased with the increasing volume fraction of hollow fillers. Wouterson[2] studied the fracture toughness of syntactic foam produced by mechanical dispersion of three different types of microspheres, Scotchlite™ K15 and K46 glass bubbles, and Phenoset BJO-093 hollow phenolic microspheres. The studies also revealed that the tensile, flexural, compressive strength of syntactic foam decreased with the increase of hollow particle content. Due to the inferior mechanical properties and low thermal conductivity, the application scope of the syntactic foam is limited.

Hollow carbon microspheres (HCMs) consist of outer stiff carbon and inner gas, which possess some common characteristics of hollow particles such as light weight, low dielectric constant and excellent sound insulation. In addition, different from HGMs, HCMs have high thermal conductivity and high specific modulus. Zhang et al. reported the mechanical properties of epoxy syntactic foams containing 30vol% HCMs with size ranging from 10-50μm lately.[16] The flexural strength and compressive yield strength of epoxy syntactic foams were comparable to that of the neat epoxy by adopting polydopamine-coated HCMs. In the previous researches, most of the syntactic foams were prepared by introducing micron scale hollow particles. The mechanical properties of polymer syntactic foams usually declined with the decreased material density, even the complicated procedures were involved to prepare and treat the fillers. If the nano-scale gas pores are introduced into the polymer matrix, the pore size is smaller than the critical dimension of cracks, which already exist in the polymer matrix, then the material density could be reduced while maintaining the essential mechanical properties.[17-19] Although the polymer foams with nano-scale pores have a lot of superior performance and could be widely applied, its preparation technologies are very limited. [19-21]

In this work, the micro and nano-scale HCMs were fabricated by template method and the HCM/epoxy syntactic foam with different HCM content and particle size was prepared. The variety in the particle size and content of HCMs brought about different impact on the mechanical properties, dimensional stability, thermal conductivity, thermal stability and dielectric properties of the resulting epoxy foam. These studies suggest that the HCM/epoxy syntactic foams may find promising applications in lightweight and high rigidity materials for advanced electronic devices.

Experiment

Material

The diglycidyl ether of bisphenol A (DGEBA, Shell EPON® 828) was used as epoxy matrix. Aromatic amine curing agents, including 3,3'-dimethyl-4,4'-diamino dicyclohexyl methane (DMDC) and diethyl methyl benzene diamine (DETDA), were obtained from Tianjin Synthetic Material Research Institute, China. The mixing ratio of DMDC and DETDA by weight was 1:2. The ratio of epoxy/amine in each system was equivalent stoichiometric to form completely cured

epoxide-amine cross-linking networks. Styrene, concentrated sulfuric acid and absolute ethyl alcohol with AR grade were purchased from Beijing Chemicals Co., China. All chemicals were used without further purification. A-stage phenol-formaldehyde resin (PF) was provided by Beijing FRP research and design institute, China.

Preparation of HCMs

The HCMs were fabricated by template method.[22] Polystyrene (PS) spheres used as templates were synthesized using emulsifier-free emulsion polymerization according to the procedure described in the literature.[23] The dry PS particles (2g) were then dispersed in 60 mL of concentrated sulfuric acid by stirring at 40 °C for 4 h, in which PS particles were modified by sulfonation, leading to the formation of sulfonic acid groups onto the surface of PS particles. After centrifugation and washing processes, 1g sulfonated PS particles were dispersed in 200mL of absolute ethyl alcohol. Subsequently, 3g of PF was diluted in 20ml absolute ethyl alcohol, and then the solution of PF was slowly dropped into the above PS mixture for 4h polymerization. The obtained PS@PF core-shell product was put into a tubular furnace, heated to 450 °C at a rate of 1 °C/min and held at this temperature for 30min to remove the PS core completely, and then to 800 °C at a rate of 2 °C/min and held at this temperature for 2 h to turn the PF shells into carbon shells. In order to investigate the influence of particle size on the physical and mechanical properties of composite, two kinds of hollow carbon microspheres with different particle size were produced, M-HCM (The particle diameter range of M-HCM is 20-100um) and N-HCM (The particle diameter range of N-HCM is about 300-500nm), as shown in Fig.1. To avoid the effect of chemical reagent on the analysis results, the purified and dried hollow carbon microspheres were used, and no other surface treatments were carried out in experiments.

Preparation of HCM/epoxy foams

For preparation of the HCM/epoxy foams, HCMs of different loading were added into the epoxy resin and the mixture was stirred at 60℃ for 3 h. Then the curing agent was added and further mixed with HCM/epoxy system at room temperature for 2h. The uniform mixture was degassed for about 15 min under vacuum conditions at 80℃. Finally, the mixture was poured into a mold,

and curing via a thermal cycle (100℃for 1 h,120℃ for 3h, 150℃ for 2h). In this work, 0.5-9 wt% of M-HCMs were added into the epoxy matrix. Considering the potential aggregation of nanoparticles in polymer matrix, only 0.5wt% and 1wt% N-HCM/epoxy samples were prepared and used for performance analysis. As a comparison, the neat epoxy samples without HCMs were cured under the same thermal cycle as that of HCM/epoxy foams.

Analysis and characterization

The morphology and surface chemical characteristics of HCMs were analyzed by using scanning electron microscopy (SEM, Hitachi S4700, Japan), transmission electron microscopy (TEM, H-800-1, Japan), Fourier transform infrared spectroscopy (FT-IR, Nexus 670, USA), Raman spectroscopy (JY-HR 800, French) and X-ray photoelectron spectroscopy (XPS, ESCALAB 250Xi, USA). The density of epoxy resin and HCM/epoxy foams was measured by an electronic densimeter (DH-300, China). Flexural properties of epoxy resin and HCM/epoxy foams were performed by using a tensile testing machine (Instron 1121, UK), according to ASTM D790. The speed of the crosshead was 1 mm/min. Compression properties of epoxy resin and HCM/epoxy foams were conducted by using a mechanical testing machine (Instron 5567, UK), according to ASTM D695. The speed of the crosshead was 1.5 mm/min. Ten specimens were measured for each case, and the average and standard deviation values were calculated. The fracture surfaces of the epoxy resin and HCM/epoxy foams were observed by SEM (Hitachi S4700, Japan). All samples were sputter-coated with gold to avoid the electric charge. The CTE value of epoxy resin and HCM/epoxy foams was measured by using a thermomechanical analyzer (TMA, TA Q400, USA) with an expansion mode at a heating rate of 5℃/min under nitrogen purge. The thermal conductivity of epoxy resin and HCM/epoxy foams was detected by a thermal conductivity analyzer (EKO HC-74, USA). The samples were cylindrical shaped, 60 mm in diameter, and 5mm in thickness. The AC resistivity and dielectric properties of epoxy resin and HCM/epoxy foams was measured in an Aligent 4294A impedance analyzer with a frequency range of 10^2–10^7 Hz at room temperature. For these measurements, silver paste was sputtered on both sides of disc-shaped samples, and the diameter of samples was 4 mm and the thickness was 0.5mm.

Results and discussion

Surface structure analysis of HCMs

The Raman spectra of M-HCMs and N-HCMs are exhibited in Fig.2. Both of the M-HCMs and N-HCMs display two characteristic peaks. The absorption peak near 1350 cm^{-1} (D band) can be assigned to the disordered graphite structures, and the absorption peak around 1580 cm^{-1} (G band) was derived from concentric cylinders of graphite layers. Although the Raman spectrum of M-HCMs showed the remarkable intensification of the D and G bands, there was no pronounced variation of peak form and location in the D and G bands between M-HCMs and N-HCMs. Furthermore, the ratio of the intensity of D band to that of G band (R value, the ratio of the integral area of corresponding peaks) can be regarded as a reasonable index to provide the quantitative information about the microstructure of carbon materials. The lower R value denotes better graphitic structure in HCMs [25]. The Raman data analysis results are presented in Table 1. The R values of M-HCM and N-HCM were very similar, which indicated that there were no significant differences between the graphitic structure in two kinds of carbon microspheres.

FT-IR spectra of the M-HCMs and N-HCMs are illustrated in Fig. 3. As shown in Fig. 3, three characteristic bands appeared at 3445 cm^{-1}, 1630 cm^{-1}, and 1120 cm^{-1}, corresponding to the O–H, C=C, and C–O stretching vibrations on the surface of both M-HCMs and N-HCMs, respectively [6]. This suggested that there existed many O–H, C=C and C–O groups on the surface of HCMs which was beneficial to the good interface bonding in the HCM/epoxy foams. In order to further approve the existence of O–H, C=C and C–O groups, the M-HCMs and N-HCMs were also examined by XPS analysis as shown in Fig.4. Both M-HCMs and N-HCMs showed C1s and O1s peaks (Fig.4 (a, c)). C1s XPS spectrum of M-HCMs and N-HCMs can be deconvoluted into two peaks with binding energies at 284.86 eV (corresponding to sp2 and sp3 hybridized carbon components (C=C/C–C)) and 285.35 eV (corresponding to C–O components) (Fig. 4(b, d)), [24] which agreed with the results of FT-IR spectroscopy.

The surface analyses of carbon microspheres indicated that there were no significant differences in both graphitic structure and chemical groups between two kinds of carbon microspheres.

Mechanical Properties of HCM/epoxy foams

The density of neat epoxy and HCM/epoxy foams was measured and shown in Fig.5. It can be seen that the density of the epoxy foams gradually declined with the increase of HCM content, due to the introduction of a large number of closed pores. Therefore, the utilization of HCM in epoxy resin can lead to lightweight foams. When 0.5wt% and 1wt% HCMs were added into the epoxy matrix, the density of M-HCM/epoxy foams with a higher volume fraction of gas pores was slightly lower than that of N-HCM filled samples.

Fig.6 shows the compression properties of neat epoxy and HCM/epoxy foams. Although the addition of hollow fillers introduced some voids and weaken the structure in the polymer matrix, the circular pores can slow down the crack damage and rigid carbon shell may also reinforce the epoxy resin. As a result, the compression strength of M-HCM/epoxy foams just decreased slightly with the increasing of M-HCM content. Compared to the neat epoxy samples, the compression strength of epoxy foams varied from 134.7MPa to 126.4MPa when M-HCMs content reached 9wt%. At the loading of 0.5wt% and 1wt % HCMs, the compression strength of N-HCM/epoxy foams was higher than that of M-HCM-filled samples, almost equivalent to the neat epoxy. At the same time, the compression modulus of M-HCM/epoxy foams was enhanced continuously with the increasing of M-HCM content. After adding 9wt% M-HCMs, the compression modulus of epoxy foams increases from 1499MPa to 1780MPa, exhibiting an enhancement of 18.7%. The HCMs in epoxy networks can effectively enhance the stiffness of the foams, leading to the increased compression modulus. When the same loading of HCMs were involved, the better reinforcing effect and stiffer epoxy foams were achieved by adding N-HCMs. This result can be attributed to the smaller particle size of the N-HCMs, which resulted in greater interfacial area and nano-level interaction between HCMs and polymer chains.

The flexural properties of neat epoxy and HCM/epoxy foams were demonstrated in Fig.7. Like compression modulus, the flexural modulus of M-HCM/epoxy foams was enhanced continuously with the increased loading of M-HCMs, which indicated the stiffness effect of the rigid HCM particles in the resulting foams.[2,10] Compared to the neat epoxy samples, the flexural modulus of 9wt% M-HCM/epoxy foams exhibited an enhancement from 2290MPa to 2675MPa,

an improvement extent of 16.8%. But at the same time the flexural strength of epoxy foams showed a downward trend with the increased M-HCM content. This phenomenon could be explained by the fact of the increased HCM amount resulting in higher void content and less effective dispersion of the particles without any chemical treatment involved. However, when the 0.5wt% and 1wt% N-HCMs were introduced into the epoxy matrix, the flexural strength of resulting foams increased to 115.9MPa and 92.3MPa, respectively, even higher than that of the neat epoxy samples. The overall interaction between the HCMs and the matrix largely depends on the surface area of the fillers. With the decrease of particle size, relative interface area between the HCMs and polymer chains increases. The nanoscale circular pores will not become weak spots in the material structure, but also can restrain the crack propagation. Therefore, the N-HCMs can impose the reinforcing function effectively in the epoxy matrix.

Fig.8 shows the fracture surface of the neat epoxy and HCM/epoxy foams after three-points bending tests. There were some regular river patterns and branches in the fracture surface of neat epoxy materials (Fig.8(a)). For M-HCM/epoxy foams, many micron scale spheres can be observed on the fracture surface. The solid patterns and branches became more sophisticated and cluttered in the fracture surface with the loading of HCMs (Fig.8(b-f)), which can provide the resistance to crack propagation. The fracture mode belonging to rigid particle reinforced-materials instead of the rupture and collapse of pores in the traditional foam plastics. As illustrated in Fig.8(g), when a crack propagated through a matrix and encountered a HCM, the crack detoured around the blockage and the deflection of the crack tip occurred after passing multiple particles. This led to a zigzag propagation path of the crack and improved the ability of polymer matrix to resist crack damage. Therefore, the introduction of HCM can reduce the material density, and also maintain or even improve the mechanical properties of polymer matrix. However, it can be seen that the carbon spheres exposed to fracture surface were clean and smooth which denotes the weak interfacial bonding between the M-HCMs and epoxy matrix. When the content of M-HCMs was higher than 5wt%, some carbon spheres began to touch each other (Fig.8(e,f)), and formed local aggregations which would diminish the reinforcement function of M-HCMs. In the 0.5wt% N-HCM/epoxy foams, most of carbon spheres were dispersed uniformly in the fracture surface of epoxy matrix (Fig.8(i)), while there was a small

amount of aggregations in the 1wt% N-HCM/epoxy samples (Fig.8(j)). As shown in the insert image of Fig.8(i), it can be noticed there existed some broken N-HCMs on the fracture surface, which meant that the nano-level interfacial bonding was stronger than that in M-HCM/epoxy foams. Compared to 1.0wt% N-HCM samples, the better reinforcing effect was achieved by adding 0.5wt% N-HCMs due to the better dispersion of nanoparticles in the polymer matrix. It is expected to further enhance the strength and modulus of the HCM/epoxy foams by adopting more effective dispersing methods and pretreatment technology of the HCMs.

Dimensional stability of HCM/epoxy foams

The dimensional stability of the neat epoxy and HCM/epoxy foams were tested and shown in Fig.9. The CTE value of the neat epoxy was $69.83\times10^{-6}/℃$ and $154.68\times10^{-6}/℃$ below and above Tg, respectively. After the HCM particles were dispersed in the epoxy matrix, these rigid additives can retard the thermal motion of the epoxy macromolecules with the rising temperature. Therefore, the addition of the HCM contributed to the decreasing thermal expansion of the epoxy foams, which led to the thermally dimensional-stable structures. With increased HCM loading, the volume fraction of epoxy resin in foams decreased accordingly, and thus, it is reasonable to observe that the CTE values of epoxy foams decreased slightly with the addition of HCM loading. When 9wt% M-HCMs were involved, the CTE values below and above Tg for the epoxy foams fell to $63.76\times10^{-6}/℃$ and $128.96\times10^{-6}/℃$. At the same time, the epoxy foams containing 0.5wt% and 1wt% N-HCMs exhibited a lower CTE value under both below and above Tg compared to that of samples with the same loading of M-HCMs. This phenomenon can also be attributed to the smaller particle size of the N-HCM, which results in the stronger interfacial interaction of the N-HCMs with the epoxy matrix.

Thermal conductivity of HCM/epoxy foams

Fig.10 reveals the thermal conductivity of HCM/epoxy foams. It can be observed that the thermal conductivity of epoxy foams showed a generally increasing trend with the enhanced content of M-HCMs up to 5 wt%. As shown Fig.10, the thermal conductivity of neat epoxy is 0.165w/mk, and then foams increased to 0.206 w/mk for the 5wt% M-HCM/epoxy samples. Because the

HCMs consist of inner gas and stiff carbon shell, the increase of the thermal conductivity of M-HCM/epoxy foams can be attributed to the high thermal conductivity of carbon shell around HCMs. [25,26] When the content of M-HCMs are beyond 5wt%, the thermal conductivity of the epoxy foams began to decline. The main reason was likely due to the increased inner gas content and degraded dispersion of the HCMs in the epoxy foams which affected the formation the effective heat transport channel.[27,28] Moreover, the scattering of phonons by interaction with the surround materials also caused the loss of thermal conduction.[29] Compared to the M-HCM/epoxy foams, the thermal conductivity of N-HCM/epoxy foams is higher at the same loading of HCMs. When the same content of the fillers was involved, the N-HCMs can provide the larger interface area with epoxy resin and transferred heat more effectively. This reflected that the size and physical characteristics of additives do have an impact on the thermal conduction of the polymer foams.

Thermal stability of HCM/epoxy foams

The thermogravimetric analyses (TGA) of HCM/epoxy foams with various HCM content and particle size were conducted in nitrogen atmosphere. Fig.11 shows TGA curves of the neat epoxy and HCM/epoxy foams. By comparing the weight loss as a function of temperature, the effect of HCMs on the thermal stability of epoxy matrix was analyzed. The TGA curves indicate that the thermal degradation of all samples consisted of only a single weight loss step between 300 and 500℃, which was in accordance with the random chain scission mechanism. It can be seen from the insert image in the Fig.11, the onset temperature of a rapid degradation region for HCM/epoxy foams was elevated slightly, compared to the neat epoxy. Under the same temperature, the thermal stability of epoxy matrix can be improved by adding HCMs. The HCMs dispersed in epoxy matrix can impose a restriction on the motion of polymer chains, and conduct heat homogeneously and avoid heat concentration. Therefore, the thermal stability of the epoxy matrix was improved by adding the HCMs. Moreover, when the particle size of the HCM decreased to nanoscale, the relative interface area between the HCMs and polymer chains increased. The N-HCMs in the epoxy resin can exert a greater restriction on the motion of polymer chains, resulting in a more effective retardation of the thermal decomposition in the

foams.[30] The dispersion of nanoscale particles in 0.5wt% N-HCM/epoxy foams was better than that in 1.0wt% N-HCM samples, and can more obviously improve the thermal stability of the resulting epoxy foams.

Dielectric properties of HCM/epoxy foams

In Fig.12, the AC conductivity, dielectric constant and dielectric loss factor of HCM/epoxy foams with different particle size and content of HCMs under various applied sweep frequencies are shown.

As revealed in Fig.12(a), the AC conductivity of M-HCM/epoxy foams rose with the increase of M-HCM content, which was attributed to the high electrical conductivity of the HCMs. When the loading of M-HCMs was lower than 7wt%, the AC conductivity displayed obvious frequency dependence which was enhanced with increasing frequency. The frequency dependence of AC conductivity of epoxy foams declined with the increase of M-HCMs. Specially, the AC conductivity of M-HCM/epoxy foams exhibited an abrupt increase as the M-HCM content increased to 7wt%. This rapid increase of AC conductivity can be attributed to the initial formation of a conducting network because the M-HCM loading was close to the percolation threshold. After the 9wt% M-HCMs was added into epoxy matrix, the AC conductivity of the resulting foams continued to increase, and remained stable value under the low frequency range. For N-HCM/epoxy foams, the AC conductivity exhibited obvious enhancement with increasing frequency after adding 0.5wt N-HCMs. When the N-HCM content was 1wt%, the AC conductivity was higher than that of 9wt% M-HCM/epoxy foams. This was because a few conducting paths deriving from aggregations of N-HCMs were formed in the epoxy resin matrix, and induced the high AC conductivity which was independent with frequency range from 10^2Hz to 10^5 Hz.[31]

From Fig.12(b), it can be seen that the dielectric constant of the neat epoxy and M-HCM/epoxy foams with low loading of M-HCMs (≤5wt%) exhibited low frequency dependence. Compared to the neat epoxy, the addition of M-HCMs initially caused a decrease of the dielectric constant. At 1MHz, the dielectric constant declined from 4.03 to 1.68 as the M-HCM content was 5wt%, because a large number of gas pores were introduced into the epoxy matrix due to the

addition of hollow fillers. However, further loading to 7wt% saw the dielectric constant of the M-HCM/epoxy foams began to sharply increase, indicating that the M-HCM loading was near the percolation threshold. The dielectric constant of epoxy foams with 7wt% and 9wt% loading of M-HCMs exhibited obvious frequency dependence which indicated the presence of an interfacial polarization in the epoxy matrix.[32] This gradually decreasing dielectric constant with increased frequency may be caused by the slow dielectric relaxation at the interface of the M-HCM/epoxy foams. Meanwhile, the N-HCM/epoxy foams showed a higher dielectric constant than that of neat epoxy, which was rising with the increased content of N-HCMs. Compared to the M-HCM/epoxy samples, the increase of the dielectric constant for N-HCM/epoxy foams could be ascribed to the interfacial polarization effect and the accumulation of charges at the nanoscale interfaces.

In Fig.12(c), when the content of M-HCMs was lower than 7wt%, the dielectric loss factor of the epoxy foams showed no obvious variations with increasing M-HCM content and sweep frequencies. After the M-HCM loading exceeded 7wt%, the loss factor rapidly increased under the low frequency range due to the initial formation of a conducting network. Because the smaller particle size of the N-HCMs, when the loading of the N-HCM reached 1wt%, the aggregation of the N-HCMs formed a few conductivity paths in the epoxy matrix. As a result, the dielectric loss of 1wt% HCM/epoxy foams was higher than that of neat epoxy and 1wt% M-HCM/epoxy foams.

Of course, the dielectric properties of the HCM/epoxy foams can be further regulated by involving different dispersed states and surface treatment of hollow particles to obtain lightweight, multifunctional polymer foams.

Conclusions

The M-HCMs and N-HCMs were fabricated by template method. The Raman spectra of M-HCM and N-HCM showed the similar graphitic structure in two kinds of carbon microspheres. FT-IR spectra and XPS analysis suggested that there exist many OH, C–O and C=C groups on the surface of HCMs, which was beneficial to the interface bonding in the HCM/epoxy foams. The HCM/epoxy syntactic foam with different HCM content and particle size was prepared. With the increasing M-HCM content, the density of the epoxy foams gradually declined, along with a decrease in compression strength and flexural strength. However, the compression modulus and

flexural modulus of M-HCM/epoxy foams were enhanced. After adding 0.5wt% and 1wt% N-HCMs, the compression strength of N-HCM/epoxy foams was almost equivalent to the neat epoxy samples, while the flexural strength of N-HCM samples exhibited an obvious superiority. For the N-HCM samples, the better reinforcing effect was achieved by adding 0.5wt% N-HCMs due to the relative uniform dispersion of nanoparticles in the polymer matrix. Similarly, compared to 1.0wt% N-HCM samples, the adding of 0.5wt% N-HCMs can more obviously improve the thermal stability of the resulting epoxy foams. The dimensional stability and thermal stability of epoxy foams was improved with the addition of HCM. The 0.5wt% and 1wt% N-HCM/epoxy foams exhibit a lower CTE value and a more effective retardation on the thermal decomposition compared to the samples with the same loading of M-HCMs. The thermal conductivity of epoxy foams showed a generally increasing trend with the M-HCM content up to 5wt%, and then begin to decline. The thermal conductivity of 0.5wt% and 1wt% N-HCM-filled foams was higher for the samples with the same loading of HCMs. The AC conductivity of M-HCM/epoxy foams exhibit an abrupt increase as the M-HCM content increased to 7wt% because the M-HCM loading was close to the percolation threshold, while the AC conductivity of 1wt% N-HCM/epoxy foams was higher than that of 9wt% M-HCM samples. Compared to the neat epoxy, the addition of M-HCMs initially caused a decrease of the dielectric constant, and a sharp increase occurred after adding 7wt% M-HCMs. In contrast, the N-HCM/epoxy foams showed a higher dielectric constant than that of neat epoxy, which could be ascribed to the interfacial polarization effect and the accumulation of charges at the nanoscale interfaces.

Acknowledgments

The authors acknowledge the financial support from the National Natural Science Foundation of China (No. 51073019), the Program for New Century Excellent Talents in University (No. NCET-12-0761) and the National High-tech R&D Program of China (863 Program) (No. 2012AA03A203).

Notes and references

[a] State Key Laboratory of Organic-Inorganic Composites, Beijing University of Chemical Technology, Beijing 100029, China

* Corresponding author, E-mail: suigang@mail.buct.edu.cn; Tel: (86)10-64427698; Fax: (86)10-64412084.

1 M. Yu, P. Zhu and Y. Ma, Effects of particle clustering on the tensile properties and failure mechanisms of hollow spheres filled syntactic foams: A numerical investigation by microstructure based modeling, *Materials and Design*, 2013, **47**, 80-89

2 E. M. Wouterso, F.Y.C. Boey, X. Hu and S. C. Wong, Specific properties and fracture toughness of syntactic foam: Effect of foam microstructures, *Composites Science and Technology*, 2005, **65**, 1840-1850

3 B. Zhu, J. Ma, J. Wang, J. Wu and D. Peng, Thermal, dielectric and compressive properties of hollow glass microsphere filled epoxy-matrix composite, *Journal of Reinforced Plastics and Composites*, 2012, **31**, 1311-1326

4 H. S. Kim and M. A. Khamis, Fracture and impact behavior of hollow micro-sphere/epoxy matrix composite, *Composite: part A*, 2001, **32**, 1311-1317.

5 H. S. Kim and P. Plubrai, Manufacturing and failure mechanisms of syntactic foam under compression, *Composite: part A*, 2004, **35**,1099-1015.

6 L. Zhang and J. Ma, Effect of coupling agent on mechanical properties of hollow carbon microsphere/phenolic resin syntactic foam, *Composites Science and Technology*, 2010, **70**, 1265-1271.

7 G. Hu and D. Yu. Tensile, Thermal and dynamic mechanical properties of hollow polymer particle-filled epoxy syntactic foam, *Materials Science and Engineering A*, 2011, **528**, 5177-5183.

8 K. C. Yung, B. L. Zhu and T. M. Yue, Preparation and properties of hollow glass microsphere-filled epoxy-matrix composites, *Composites Science and Technology*, 2009, **69**(2), 260-264.

9 S. J. Park, F. L. Jin and C. Lee, Preparation and physical properties of hollow glass microspheres-reinforced epoxy matrix resins, *Materials Science and Engineering: A*, 2005, **402**(1), 335-340.

10 G. Tagliavia, M. Porfiri and N. Gupta, Analysis of flexural properties of hollow-particle filled composites, *Composites: Part B*, 2010, **41**, 86-93.

11 N. Gupta and R. Nagorny, Tensile properties of glass microballoon-epoxy resin syntactic foams, *Journal of Applied Polymer Science*, 2006, **102**, 1254-1261.

12 N. Gupta, S. Kumar Gupta and B. J. Mueller, Analysis of a functionally graded particulate composite under flexural loading conditions, *Materials Science and Engineering A*, 2008, **485**, 439-447.

13 N. Gupta, R. Ye and M. Porfiri. Comparison of tensile and compressive characteristics of vinyl ester/glass microballoon syntactic foams, *Composites: Part B*, 2010, **41**, 236-245.

14 N. Gupta, Eyassu Woldesenbet, Patrick Mensah. Compression properties of syntactic foams: effect of cenosphere radius ratio and specimen aspect ratio. Composites: Part A, 2004, **35**: 103-111.

15 M. Porfiri and N. Gupta, Effect of volume fraction and wall thickness on the elastic properties of hollow particle filled composites, *Composites Part B: Engineering*, 2009, **40**, 166-173.

16 L. Zhang, S. Roy, Y. chen, E. K. Chua, K. Y. See, X. Hu and M. Liu, Mussel-inspired polydopamine coated hollow carbon microspheres, a novel versatile filler for fabrication of high performance syntactic foams, *ACS Applied Materials & Interfaces*, 2014, **6**, 18644-18652.

17 Y. Ema, M. Ikeya and M. Okamoto, Foam processing and cellular structure of polylactidebased nanocomposites, *Polymer*, 2006, **47**, 5350-5359.

18 L. J. Lee, C. Zeng, X. Cao, X. Han, J. Shen and G. Xu, Polymer nanocomposite foams, *Composites Science and Technology*, 2005, **65**, 2344-2363.

19 C. Zeng, X. Xan, L. J. Lee, K. W. Koelling and D. L. Tomasko. Polymer-clay nanocomposite foams prepared using carbon dioxide, *Advanced Materials*, 2003, **15**, 1743.

20 Y. Ema, M. Ikeya and M. Okamoto. Foam processing and cellular structure of polylactidebased nanocomposites, *Polymer*, 2006, **47**, 5350-5359.

21 L. J. Lee, C. Zeng, X. Cao, X. Han, J. Shen and G. Xu, Polymer nanocomposite foams, *Composites Science and Technology*, 2005, **65**, 2344-2363.

22 M. Yang, J. Ma, S. J. Ding, Z. K. Meng, J. G. Liu, T. Zhao, L. Q. Mao, Y. Shi, X. G. Jin, X. F. Lu and Z. Z. Yang, Phenolic resin and derived carbon hollow spheres. *Macromolecular Chemistry and Physics*, 2006, **207**(18): 1633-1639.

23 S. X. Chen, X. Zhang and P. K. Shen. Macroporous conducting matrix: Fabrication and application as electrocatalyst support, *Electrochemistry Communications*, 2006, **8**, 713-719.

24 W. Lee, J. U. Lee, B. M. Jung, J. H. Byun, J. W. Yi, S. B. Lee and B. S. Kim, Simultaneous enhancement of mechanical, electrical and thermal properties of graphene oxide paper by embedding dopamine, *Carbon*, 2013, **65**, 296-304.

25 H. Lei Y. Wang and J. Huo, Porous graphitic carbon materials prepared from cornstarch with the assistance of microwave irradiation, *Microporous and Mesoporous Materials*, 2015, **210**, 39-45.

26 A. Stein, Z. Wang and M. A. Fierke, Functionalization of porous carbon materials with designed pore architecture, *Adv. Mater.*, 2009, **21**, 265-293.

27 K. Yang, M. Gu, Y. Guo, X. Pan and G. Mu. Effects of carbon nanotube functionalization on the mechanical and thermal properties of epoxy composite, *Carbon*, 2009, **47**, 1723-1737.

28 W. Cui, F. Du, J. Zhao, W. Zhang, Y. Yang, X. Xie and Y. Mai. Improving thermal conductivity while retaining high electrical resistivity of epoxy composites by incorporating silica-coated multi-walled carbon nanotubes, *Carbon*, 2011, **49**, 495-500.

29 M. Moniruzzaman and K. I. Winey, Polymer Nanocomposites Containing Carbon Nanotubes, *Macromolecules*, 2006, **39**, 5194-5205.

30 W. J. Wang, C. W. Li and K. P. Chen. Electrical, dielectric and mechanical properties of a novel Ti3AlC2/epoxy resin conductive composites, *Materials Letters*, 2013, **110**, 61-64.

31 L. L. Sun, Y. Zhao and W. H. Zhong, Dependence of dielectric properties and percolative behavior on phase separation structure induced by heterogeneous carbon nanofiber distribution in polymer blend nanocomposites. *Macromolecular Materials and Engineering*, 2011, **296**, 992-1001.

32 A. R. Luxmoore and D. R. J. Owen, The mechanics of cellular plastics, *Applied Science Publishers*, Barking, 1980, pp. 359-391.

Table captions

Table 1 Data analysis in Raman spectra of M-HCMs and N-HCMs

Figure captions

Fig.1 Microstructure of M-HCMs and N-HCMs: (a) SEM image and partial enlarged photograph (shown as the insert images) of M-HCMs; (b) SEM image and TEM image (shown as the insert images) of N-HCMs

Fig.2 Raman spectra of M-HCMs and N-HCMs

Fig.3 FT-IR spectra of M-HCMs and N-HCMs

Fig.4 XPS spectra of M-HCMs and N-HCMs: (a) wide scan spectra of M-HCMs; (b) C1s spectrum of M-HCMs with deconvoluted peaks; (c) wide scan spectra of N-HCMs; (d) C1s spectrum of N-HCMs with deconvoluted peaks

Fig.5 Density of neat epoxy and HCM/epoxy foams

Fig.6 The compression properties of neat epoxy and HCM/epoxy foams: (a) compression strength; (b) the compression modulus

Fig.7 The flexural properties of neat epoxy and HCM/epoxy foams: (a) flexural strength; (b) flexural modulus

Fig.8 The fracture morphology of neat epoxy and HCM/epoxy foams: (a) neat epoxy; (b) 0.5wt% M-HCM/epoxy foams; (c) 1wt% M-HCM/epoxy foams; (d) 3wt% M-HCM/epoxy foams; (e) 5wt% M-HCM/epoxy foams; (f) 7wt% M-HCM/epoxy foams; (g) 9wt% M-HCM/epoxy foams; (h) the crack propagation in 5wt% M-HCM/epoxy foams; (i) 0.5wt% N-HCM/epoxy foams; (j) 1wt% N-HCM/epoxy foams (small aggregation of N-HCMs was shown in the insert image)

Fig.9 CTE values of neat epoxy and HCM/epoxy foams below and above Tg

Fig.10 The thermal conductivity of neat epoxy and HCM/epoxy foams

Fig.11 TGA curves of neat epoxy and HCM/epoxy foams

Fig.12 Dielectric properties of neat epoxy and HCM/epoxy foams: (a) AC conductivity; (b) dielectric constant; (c) dielectric loss factor

Table 1 Data analysis in Raman spectra of M-HCMs and N-HCMs

	The integral area of D band	The integral area of G band	R
M-HCMs	3.23×10^{6}	1.35×10^{6}	2.39
N-HCMs	1.38×10^{6}	5.63×10^{5}	2.45

Fig.1

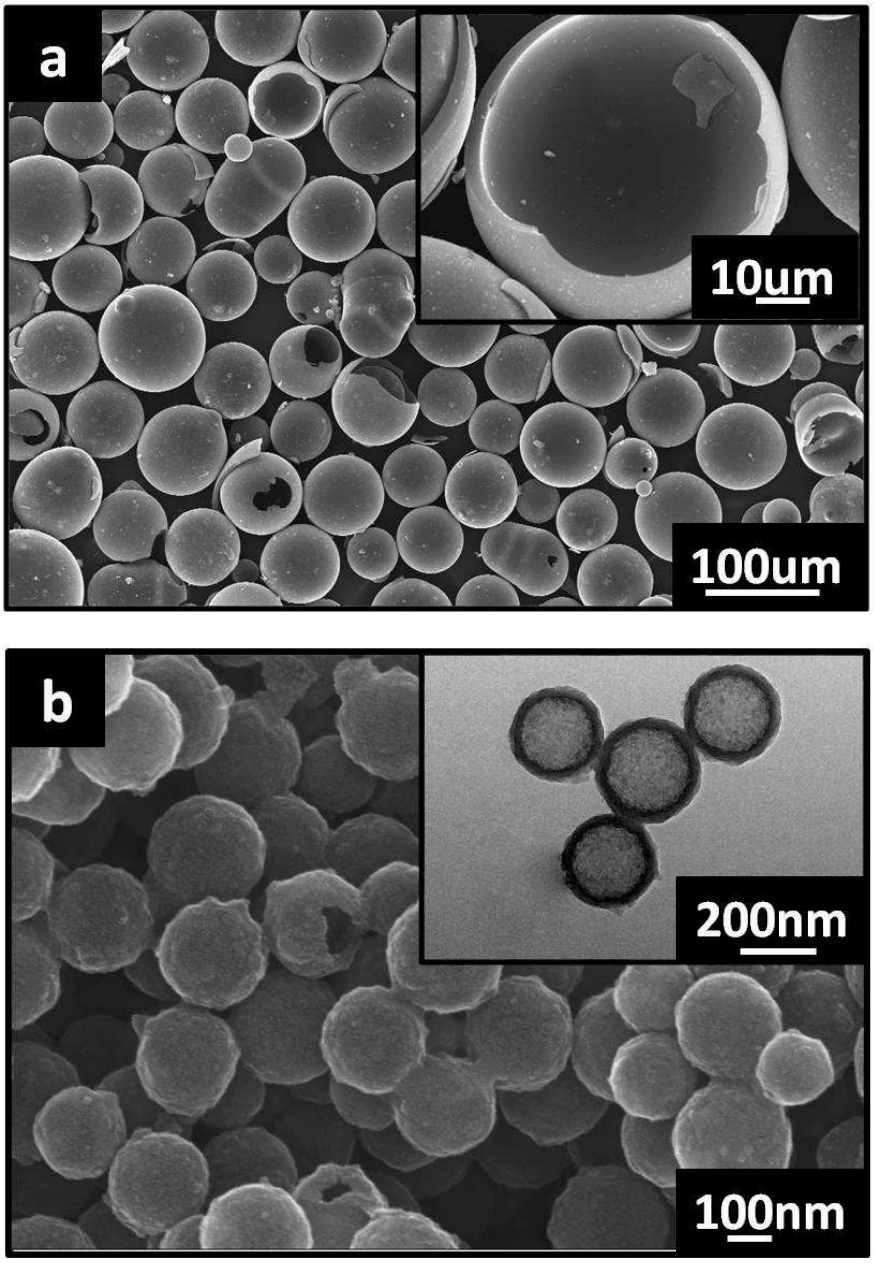

Fig.2

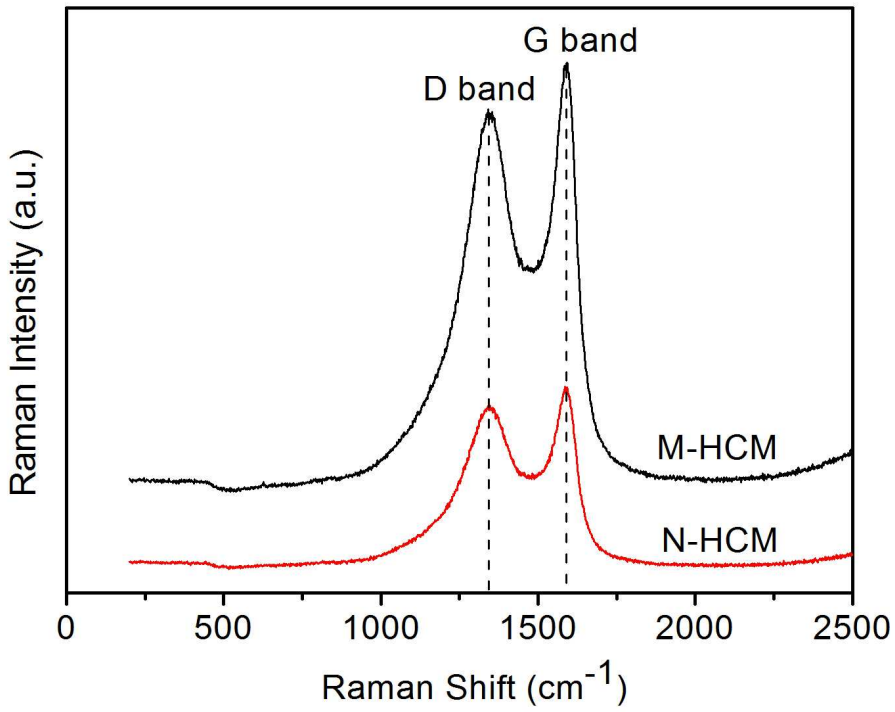

Fig.3

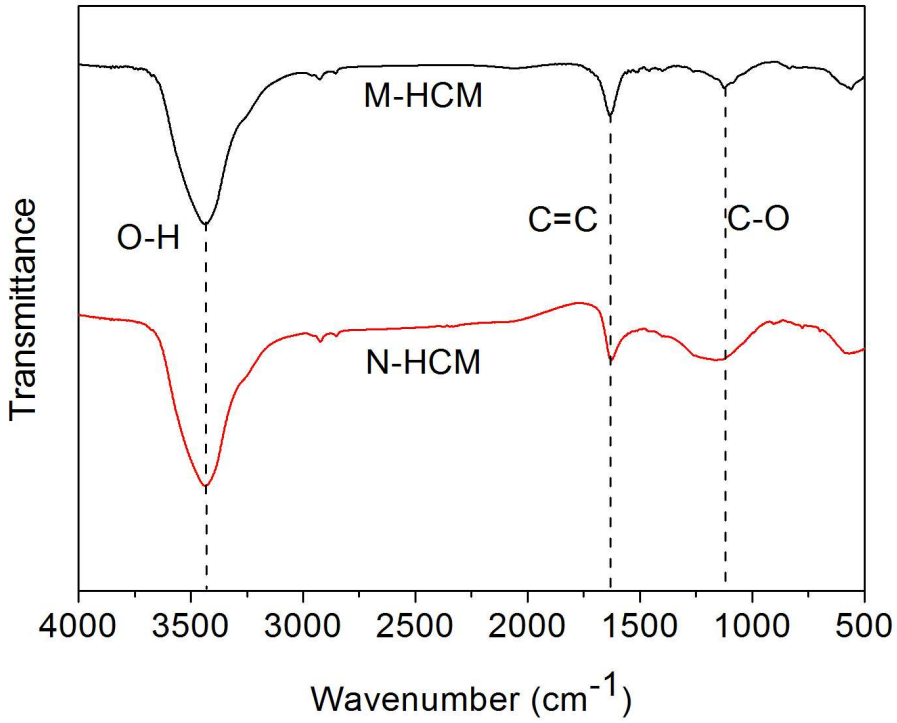

Fig.4

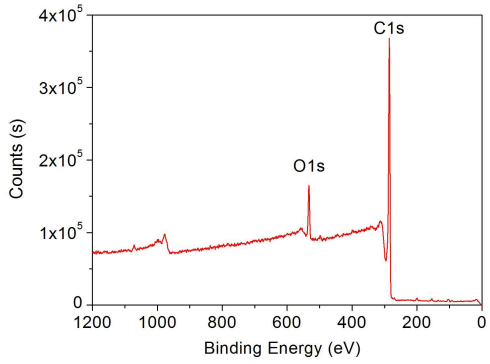

(a)

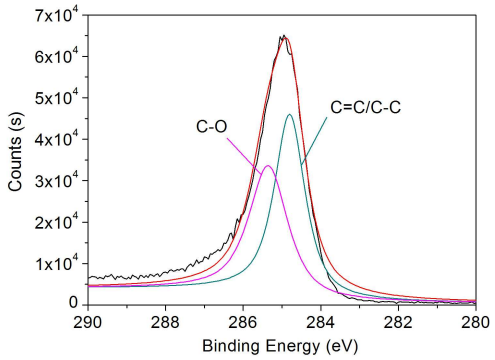

(b)

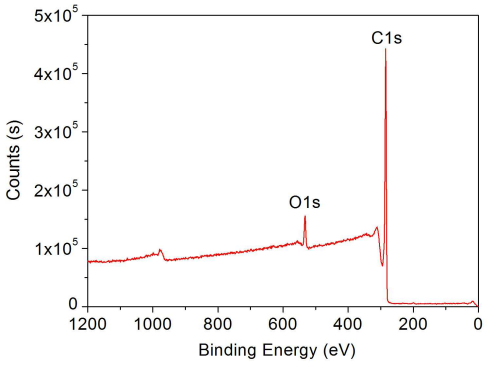

(c)

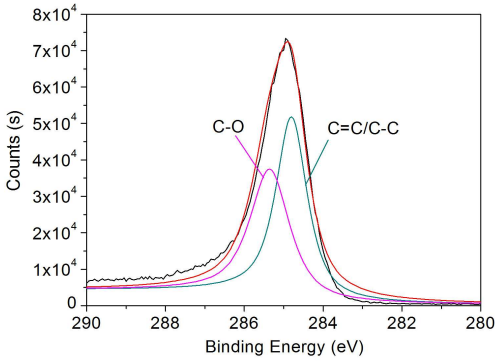

(d)

Fig.5

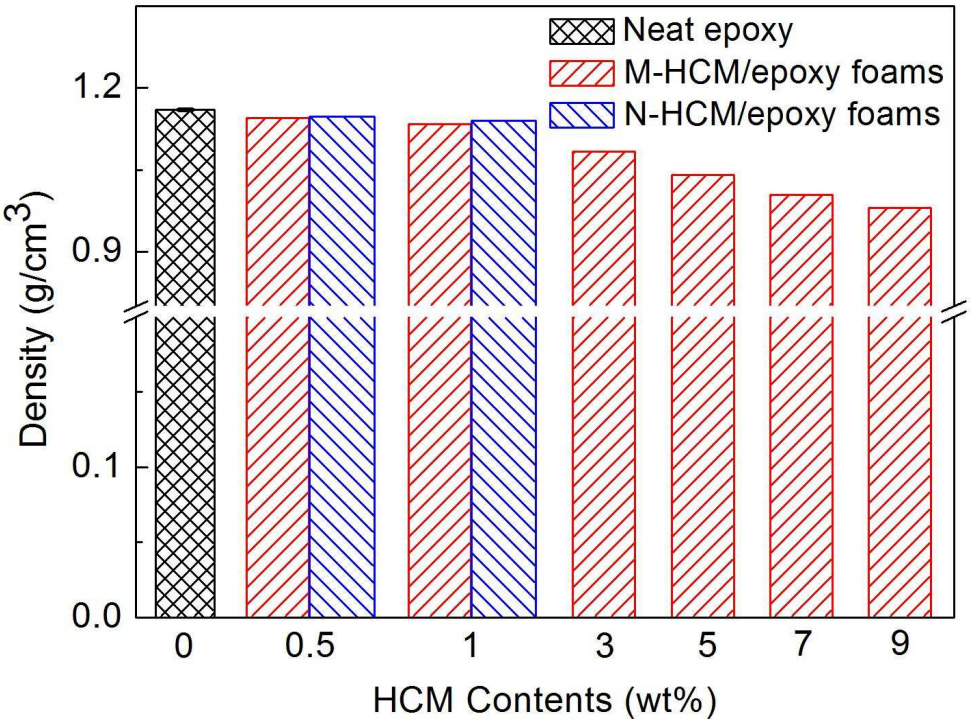

Fig.6

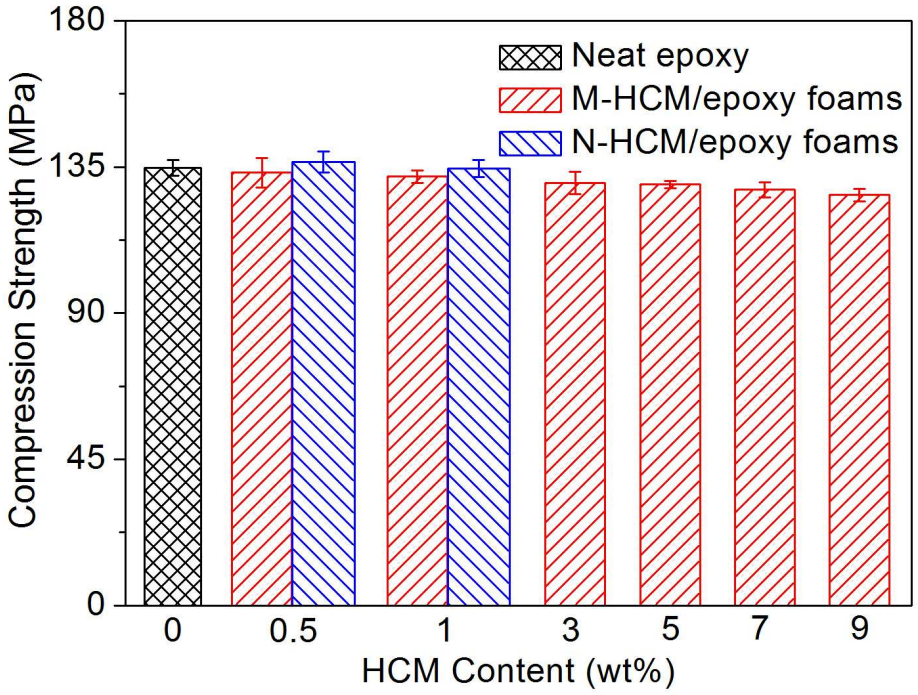

(a)

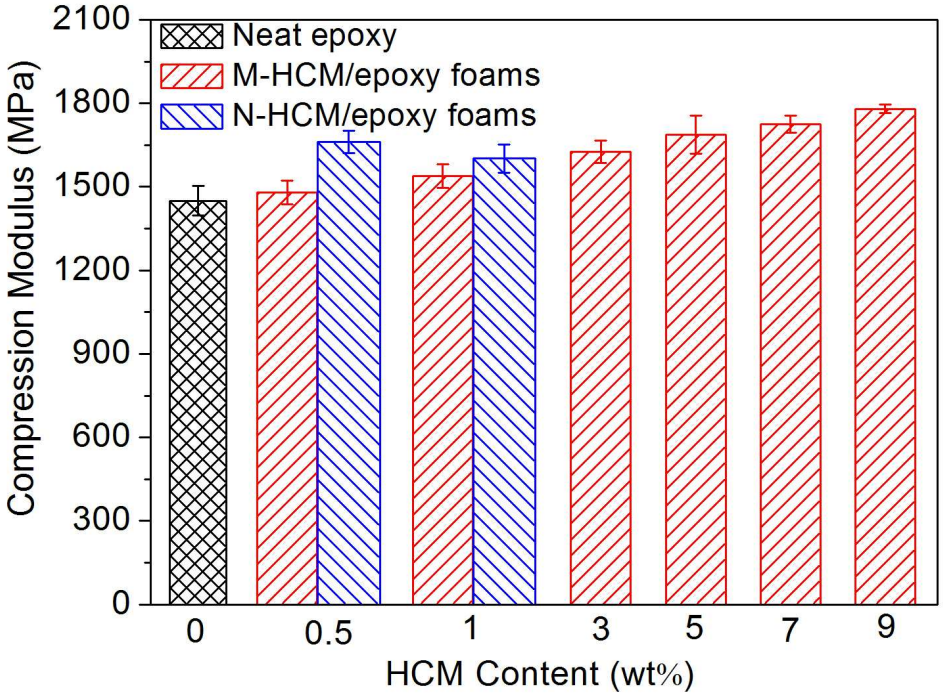

(b)

Fig.7

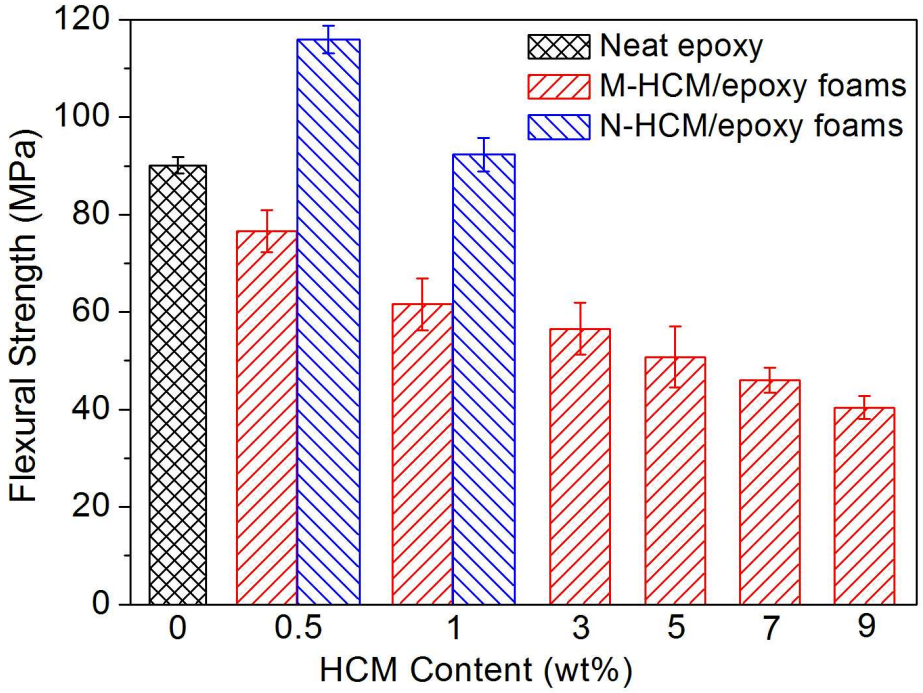

(a)

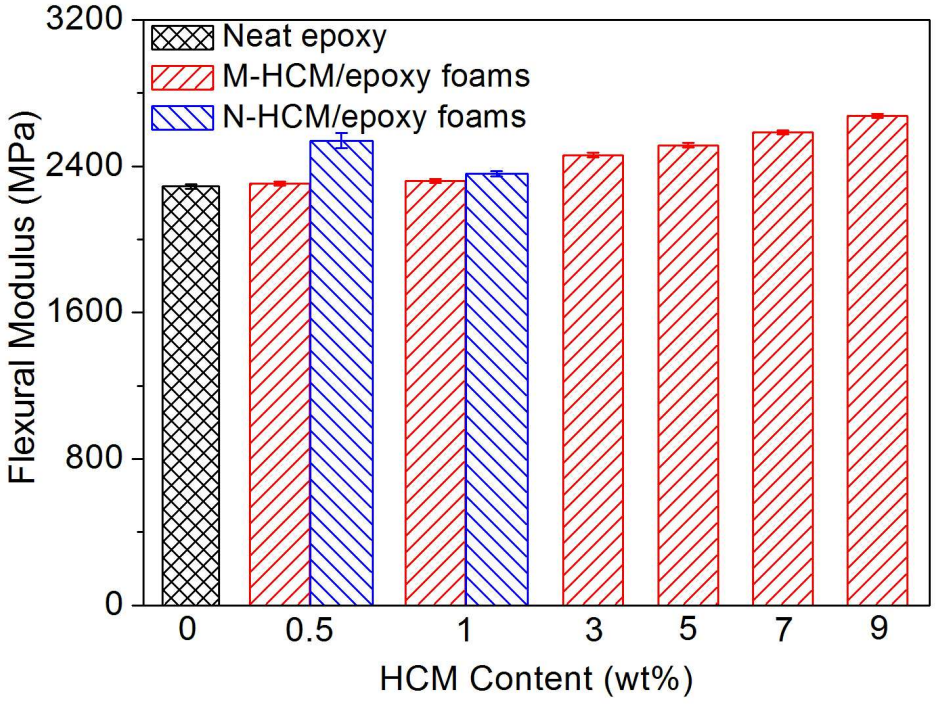

(b)

Fig.8

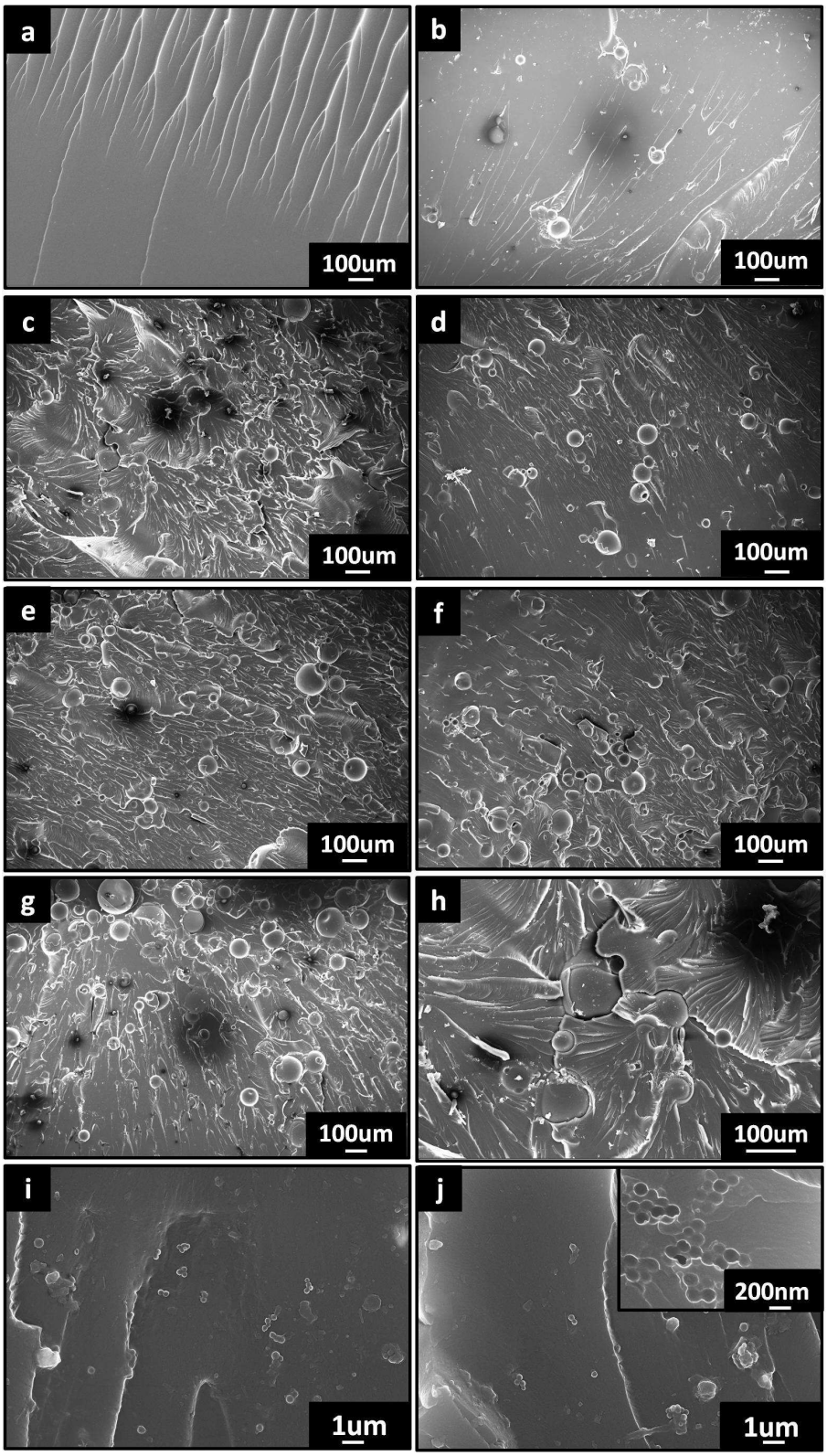

Fig.9

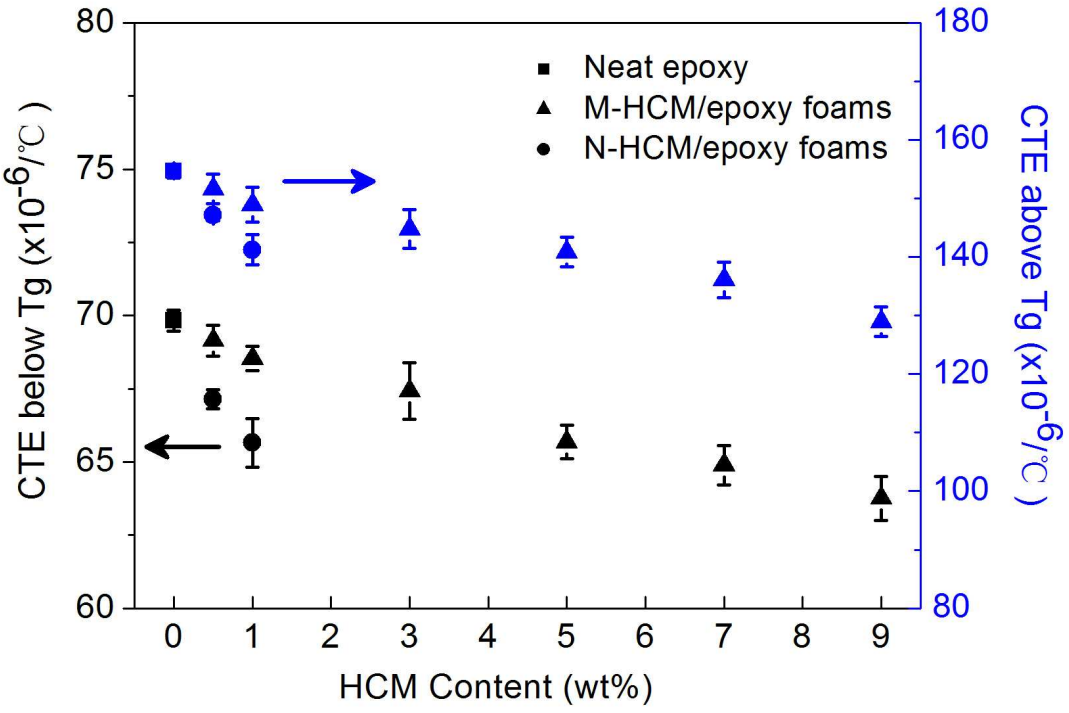

Fig.10

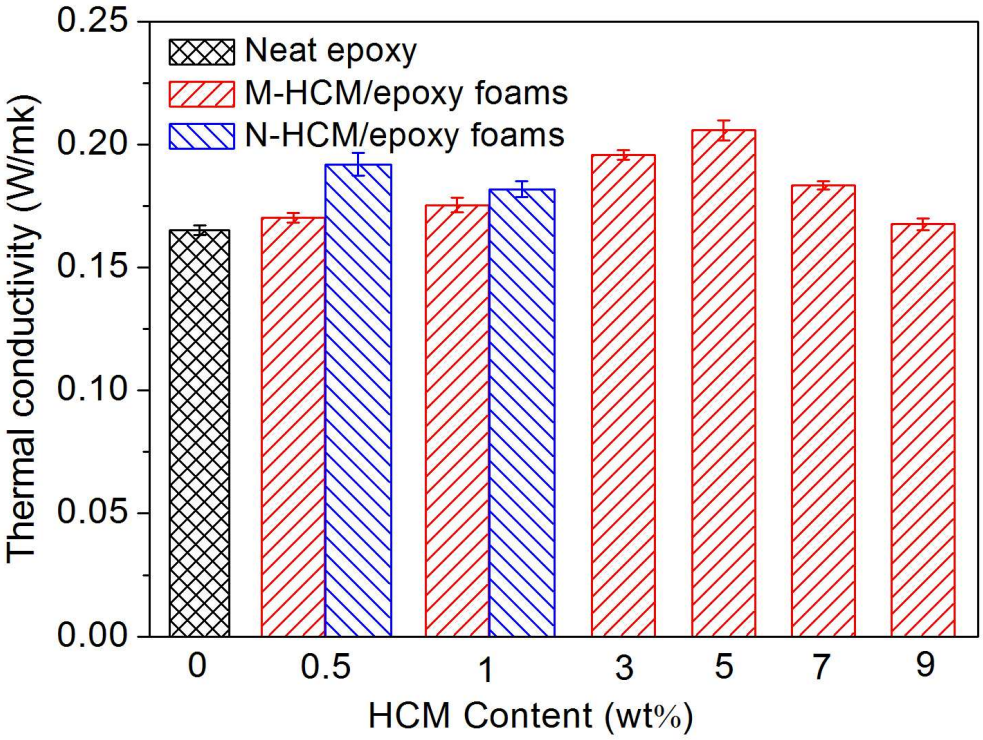

Fig.11

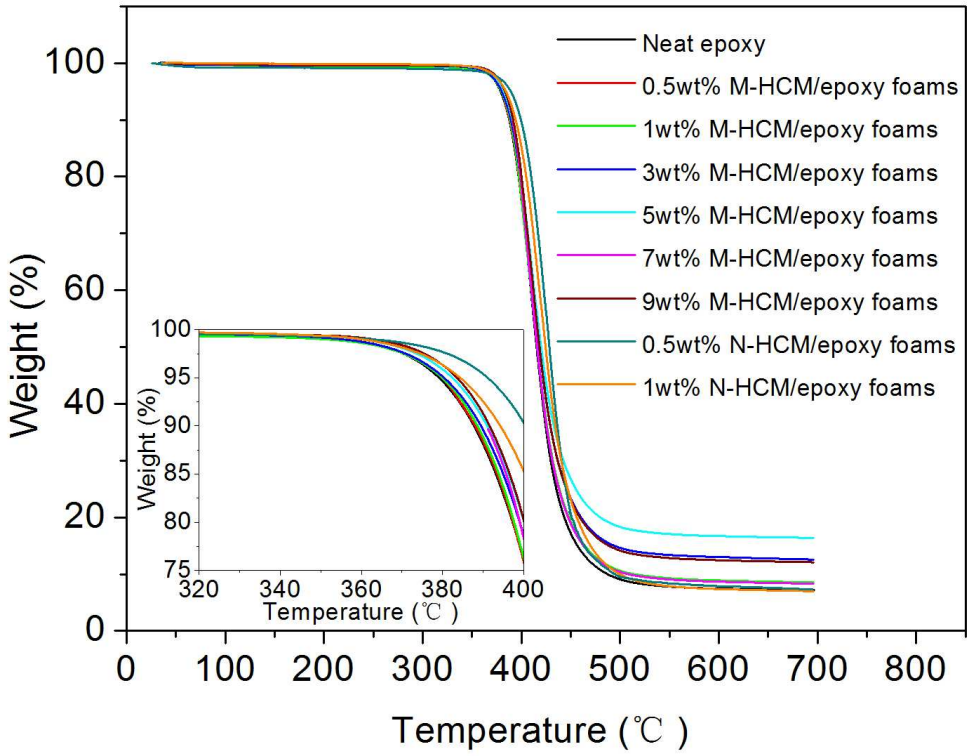

Fig.12

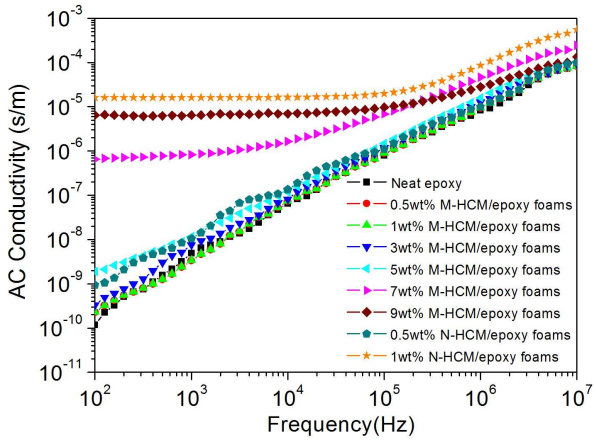

(a)

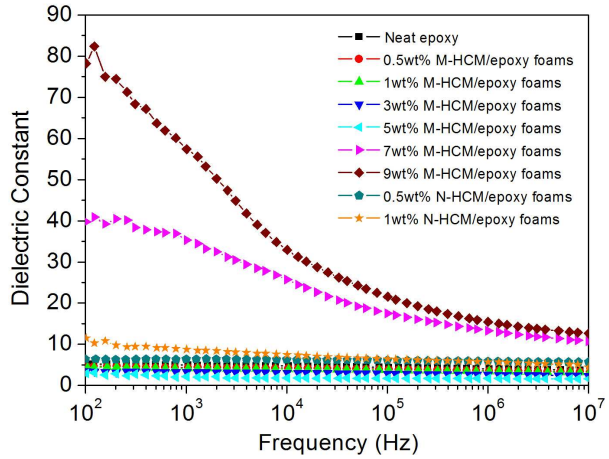

(b)

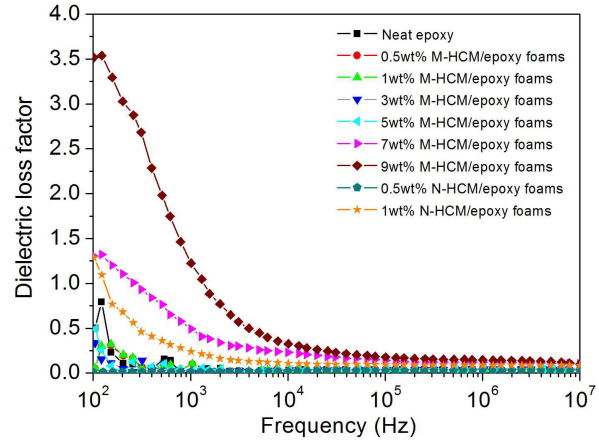

(c)